SAND2016-9617R

Dynamics and Solubility of He and CO_2 in Brine

Tuan A. Ho[1] **and Craig Tenney**[2]

[1]*Geochemistry Department, Sandia National Laboratories, Albuquerque, New Mexico 87185, USA.*

[2]*WMD Threats and Aerosol Science, Sandia National Laboratories, Albuquerque, New Mexico 87185, USA.*

This research is conducted in an effort to collaborate with Baole Wen and Marc Hesse at UT to study the effect of convection on the solubility and dynamics of gas in brine at Bravo Dome natural gas field. Below we summarize the method and results for the study of dynamics and solubility of He and CO_2 in NaCl aqueous solution.

1. Dynamics of gas in NaCl aqueous solution

a. Method

Molecular dynamics simulation was implemented using LAMMPS simulation package (1) to study the diffusivity of He^3 and CO_2 in NaCl aqueous solution. To simulate at infinite dilute gas concentration, we placed one He^3 or CO_2 molecule in an initial simulation box of 24x24x33Å^3 containing 512 water molecules and a certain number of NaCl molecules depending on the concentration. Initial configuration was set up by placing water, NaCl, and gas molecules into different regions in the simulation box. Calculating diffusion coefficient for one He or CO_2 molecule consistently yields poor results. To overcome this, for each simulation at specific conditions (i.e., temperature, pressure, and NaCl concentration), we conducted 50 simulations initiated from 50 different configurations. These configurations are obtained by performing the simulation starting from the initial configuration mentioned above in the NVE ensemble (i.e., constant number of particles, volume, and energy). for 100,000 time steps and collecting one configuration every 2,000 times step. The output temperature of this simulation is about 500K. The collected configurations were then equilibrated for 2ns in the NPT ensemble (i.e., constant number of particles, pressure, and temperature) followed by 9ns simulations in the NVT ensemble (i.e., constant number of particles, volume, and temperature). The time step is 1fs for all simulations.

We focused on studying the diffusivity of He and CO_2 in brine at the conditions relevant to those found at the Bravo Dome CO_2 gas field in New Mexico (2). For example, the pressure varies from 2 MPa to 14 MPa depending upon the location at Bravo Dome. Temperature is from 300K to 320K, and NaCl concentration is about 0.4 mol/l (3). In our simulation, we varied NaCl concentration from 0 to 4 mol/l to study the effect of salinity on the diffusion coefficient. Water molecule was simulated using the SPC/E model (4). This water model can properly predict the diffusion coefficient of bulk water (5). The He molecule was modeled as a Lennard-Jones sphere with the potential parameters taken from Tang and Toennies (6). The CO_2 molecule was described by the TRaPPE model (7) and kept rigid using an algorithm proposed by Kamberaj et al. (8). The NaCl force field was adopted using the SD model proposed by Smith and Dang (9). The cross-interaction between He and water molecules was taken from Warr et al. (10). Other unlike-pair parameters were computed using the Lorentz-Berthelot combining rule rules $\varepsilon_{ij} = \sqrt{\varepsilon_{ii}\varepsilon_{jj}}$ and $\sigma_{ij} = (\sigma_{ii} + \sigma_{jj})/2$, where ε and σ are the depth of the potential well and the distance at which inter-particle the potential is zero in the Lennard-Jones potential, respectively.

Diffusion coefficient *D* was calculated by using Einstein relation (11) $D = \lim_{t\to\infty} \frac{\langle [x(t)-x(0)]^2 \rangle}{6t}$, where $[x(t) - x(0)]$ is the distance from the starting point at time *t* = *0* that molecule diffuses in time *t*. Trajectories of He, CO_2, and water obtained in 9ns NVT simulations are divided into 3 blocks of 3ns each. The mean square displacement (i.e., numerator in the Einstein relation) was averaged from 50 simulations for each block and used to compute the diffusion coefficient. Finally, the mean value of the diffusion coefficient and the standard deviation were calculated from the result obtained for each block. To validate our methodology and models, we compared the diffusion coefficient of CO_2 and He in pure water at 300K and 1atm with those available in literature. The diffusion coefficient of CO_2 in water obtained from our simulation is $1.83 \pm 0.44 \times 10^{-9} m^2/s$, which is in agreement with that calculated by Moultos (12) ($2.2 \pm 0.5 \times 10^{-9} m^2/s$) and experimental results (13). The diffusion coefficient of He in pure water calculated from our simulation is $7.06 \pm 0.75 \times 10^{-9} m^2/s$, which is comparable with the experimental data by Jahne (14) ($D = 7.22 \pm 0.36 \times 10^{-9} m^2/s$).

b. Results

In the left panel of Figure 1 we present the diffusion coefficient of CO_2 and He in 0.44mol/l NaCl solution at 0.1MPa as a function of temperatures ranging from 300 to 340K. As expected, when the temperature increases, the diffusion coefficient increases for He, CO_2, and water. The ratio of the diffusion coefficient of He/CO_2 is from 2.69 to 3.45. We also observed that the diffusion coefficient of dissolved CO_2 is comparable with that of water. Note that dissolved CO_2 is coordinated by around 19 water molecules (15). Therefore, the diffusivity of CO_2 strongly depends on the movement of the surrounding water molecules. On the other hand, the diffusion coefficient of solute He is much higher than those of water and dissolved CO_2, in part, because He mass is smaller and because water does not form a strong hydration shell around He.

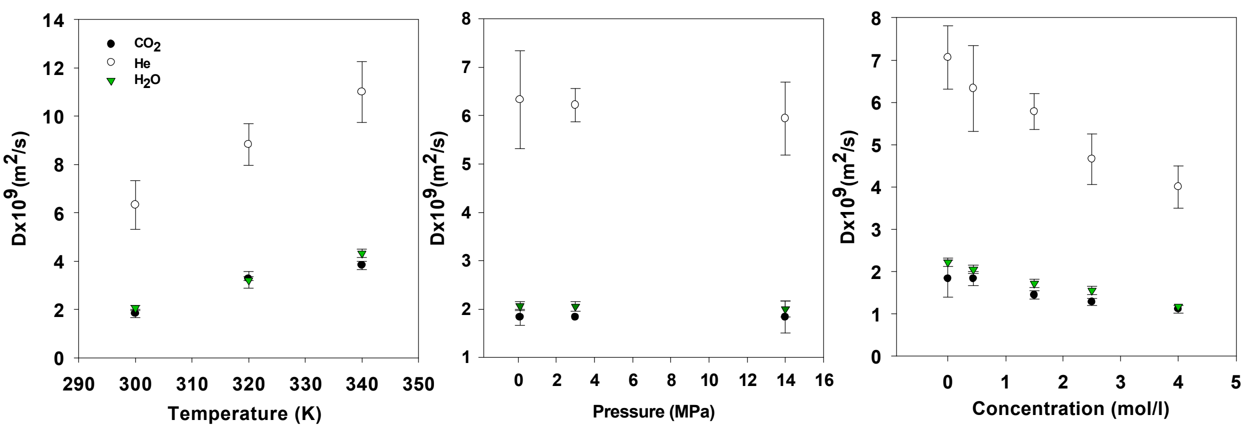

Figure 1. Diffusion coefficient of CO_2 (solid circles), water (triangles), and He (empty circles) as a function of temperature (left), pressure (middle), and salt concentration (right). The NaCl concentration is 0.44 mol/l for the left and middle panels. The pressure is 0.1MPa for the left and right panels. The temperature is 300K for the middle and right panels.

In the middle panel of Figure 1 we report the diffusion coefficient as a function of pressure ranging from 0.1 to 14MPa. The temperature is 300K and NaCl concentration is 0.44m/l. Our results indicate that the pressure change observed at Bravo Dome does not affect the mobility of gas in NaCl aqueous solution. This is expected because water is incompressible and its diffusion coefficient does not change as a function of pressure. In the right panel of Figure 1 we present the diffusion coefficients of water, He and CO_2 as a function of NaCl concentration increasing from 0 to 4 mol/l. The temperature is 300K and pressure is 0.1MPa. The results suggest that diffusion coefficients of water, CO_2 and He decrease when NaCl concentration increases. This observation is in agreement with experiment (16). As the number of Na^+ and Cl^- ions increases, more water molecules bind to Na^+ and Cl^- ions to form the ion-water cluster. These clusters diffuse more slowly than water. Because the diffusion coefficient of water decreases when increasing NaCl concentration, the diffusion coefficients of dissolved CO_2 and He decrease.

2. Solubility of CO_2 and He in NaCl aqueous solution

a. Method

The NPT-Gibbs ensemble (17) Monte Carlo (MC) simulation was conducted using TOWHEE simulation package (18) to study the solubility of CO_2 and He in an NaCl aqueous solution. In our simulation setup there are two simulation boxes: the liquid box containing 512 water molecules and a certain number of NaCl depending on the concentration, and the gas box containing 512 gas molecules (either CO_2 or He). These two boxes were kept at a constant temperature and pressure. During the course of simulation, liquid/gas phase equilibrium was obtained by the molecule exchanges between two boxes. In addition, the equilibration in each phase is carried out by molecule movement (i.e., translational and rotational moves) and reinsertion move. After each MC move, the potential energy of the system was calculated and used in the Metropolis algorithm (19) to decide if the move was accepted. Our simulations were carried out for 180 million steps. The last 120 million steps were divided into 10 blocks of 12 million steps each to calculate the mole fraction of gas in the brine and standard deviation.

For the He/NaCl aqueous system, we implemented the same potential energy for water, He, and NaCl as we did in the study of the diffusion coefficient. The Henry's constant of He in pure water obtained from our simulation is 16.1±3.4GPa at 300K and 0.1MPa. This is consistent with the experimental result (14.6 ± 1.4 GPa)(20). For the CO_2/brine system, following Vorholz et al. (21), we used the SPC model (22) for water and EPM2 (23) model for CO_2. The SPC water model yields a better prediction of vapor pressure than most water models (24). When simulating EPM2 CO_2 the unlike-pair interaction between carbon and oxygen atoms was calculated by using the geometric combining rules $\varepsilon_{CO} = \sqrt{\varepsilon_{CC}\varepsilon_{OO}}$ and

$\sigma_{CO} = \sqrt{\sigma_{CC}\sigma_{OO}}$, where ε and σ are the depth of the potential well and the distance at which inter-particle the potential is zero in the Lennard-Jones potential, respectively. Other unlike-pair parameters were calculated by using Lorentz-Berthelot rules $\varepsilon_{ij} = \sqrt{\varepsilon_{ii}\varepsilon_{jj}}$ and $\sigma_{ij} = (\sigma_{ii} + \sigma_{jj})/2$. In Figure 2 we compare our results with the simulation results by Vorholz et al. (21) and experimental data by Hou et al. (25) to validate our methodology. Agreement between our simulation data with those by Vorholz et al. (21) is observed within the statistical uncertainties (smaller error bar in our results probably is because our simulations are longer). Comparison also indicates that simulation underestimates the solubility of CO_2 in pure water, especially at high pressure, possibly because of the inadequacy of the combining rules. However, the trend of the effect of the temperature, pressure and NaCl concentrations on the solubility can be studied using these models.

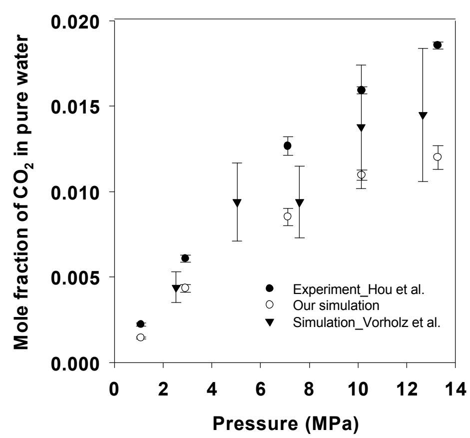

Figure 2. Mole fraction of CO_2 in pure water at 348.15K and 1 atm. Comparisons of our results (empty circles) with simulation results by Vorholz et al. (21) (triangles) and experimental data by Hou et al. (25) (solid circles).

b. Results

In the top left panel of Figure 3 we present the mole fraction of He in an NaCl aqueous solution when the temperature changes from 290K to 340K. The pressure is 3MPa and NaCl concentration is 0.44 mol/l. The results indicate that within the narrow temperature range at Bravo Dome, the solubility of He into the aqueous solution does not change significantly. However, pressure variation at Bravo Dome (i.e., from 2 to 14MPa) remarkably affects the solubility of He (top middle panel of Figure 3). The He solubility increases up to 2 orders of magnitude when pressure increases from 0.1MPa to 14MPa. The concentration of NaCl also significantly affects the solubility of He (top right panel of Figure 3). The He solubility decreases up to 1 order of magnitude when the NaCl concentration increases from 0.44 mol/l (i.e, Bravo Dome NaCl concentration) to 4.0 mol/l.

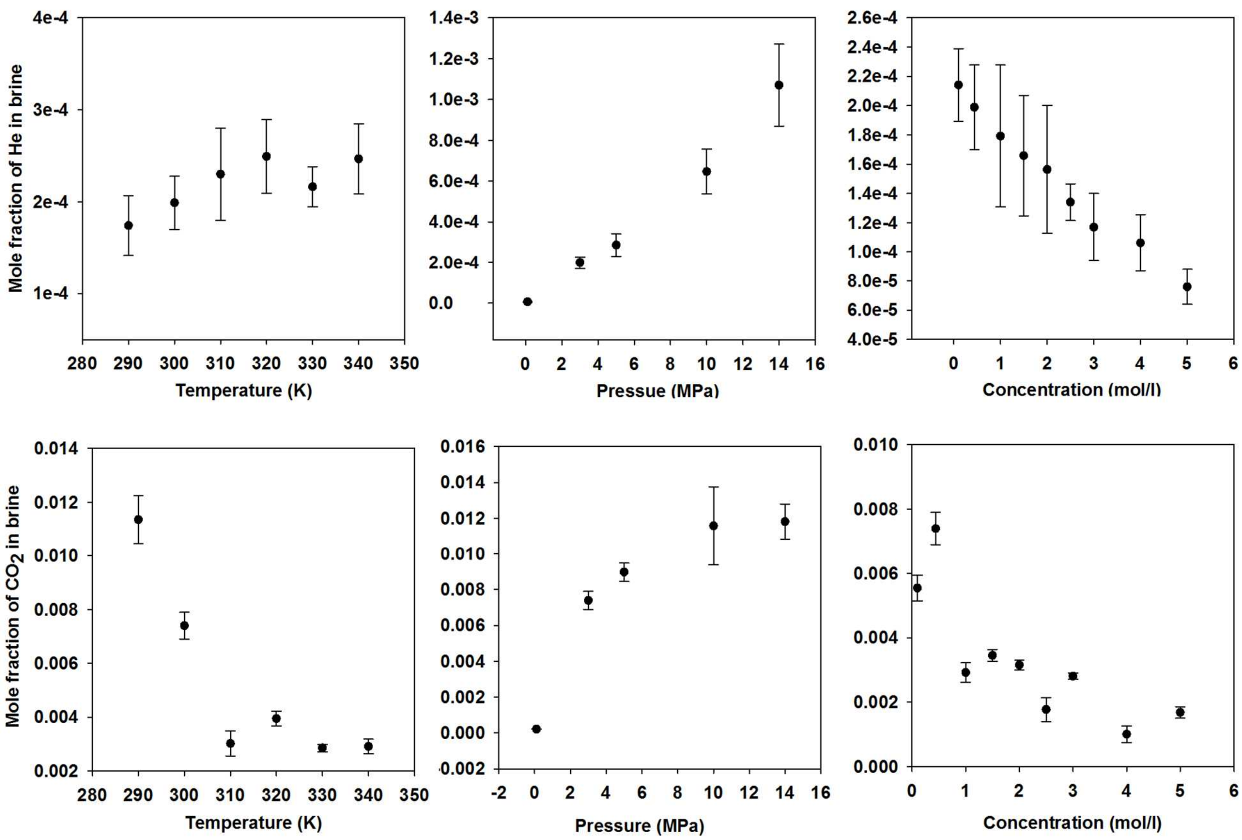

Figure 3. Mole fraction of He (top panels) and CO_2 (bottom panels) in an NaCl aqueous solution as a function of temperature (left panels), pressure (middle panels) and NaCl concentration (right panels). The NaCl concentration is 0.44 mol/l for left and middle panels. The pressure is 3MPa for the left and right panels. The temperature is 300K for middle and right panels.

In the bottom left panel of Figure 3 we report the mole fraction of CO_2 in NaCl aqueous solution as a function of temperature varying from 290K to 340K. The effect of the temperature on the solubility of CO_2 is more significant when compared with the result for He. The solubility of CO_2 decreases when temperature increases. The results shown in the bottom middle panel of Figure 3 indicate that when pressure increases, the solubility of CO_2 increases, as expected. This observation suggests that at a different location at the Bravo Dome, the solubility of CO_2 in brine might be different. We also observed that, because of the salting out effect, when the NaCl concentration increases, the solubility of CO_2 decreases. As ions electrostrict water molecules in the hydration shell, increasing the number of ions in the solution reduces the number of water molecules available to coordinate with gas molecules (3).

Acknowledgement

Sandia National Laboratories is a multi-program laboratory managed and operated by Sandia Corporation, a wholly owned subsidiary of Lockheed Martin Corporation, for the U.S. Department of Energy's National Nuclear Security Administration under contract DE-AC04-94AL85000

References

1. Plimpton S (1995) Fast Parallel Algorithms for Short-Range Molecular-Dynamics. *J Comput Phys* 117(1):1-19.
2. Sathaye KJ, Hesse MA, Cassidy M, & Stockli DF (2014) Constraints on the magnitude and rate of CO2 dissolution at Bravo Dome natural gas field. *P Natl Acad Sci USA* 111(43):15332-15337.
3. Gilbert K, Bennett PC, Wolfe W, Zhang T, & Romanak KD (2016) CO2 solubility in aqueous solutions containing Na+, Ca2+, Cl−, SO42− and HCO3-: The effects of electrostricted water and ion hydration thermodynamics. *Applied Geochemistry* 67:59-67.
4. Berendsen HJC, Grigera JR, & Straatsma TP (1987) The Missing Term in Effective Pair Potentials. *J Phys Chem-Us* 91(24):6269-6271.
5. Mark P & Nilsson L (2001) Structure and dynamics of the TIP3P, SPC, and SPC/E water models at 298 K. *J Phys Chem A* 105(43):9954-9960.
6. Tang KT & Toennies JP (1986) New Combining Rules for Well Parameters and Shapes of the Van Der Waals Potential of Mixed Rare-Gas Systems. *Z Phys D Atom Mol Cl* 1(1):91-101.
7. Potoff JJ & Siepmann JI (2001) Vapor-liquid equilibria of mixtures containing alkanes, carbon dioxide, and nitrogen. *Aiche J* 47(7):1676-1682.
8. Kamberaj H, Low RJ, & Neal MP (2005) Time reversible and symplectic integrators for molecular dynamics simulations of rigid molecules. *Journal of Chemical Physics* 122(22).
9. Smith DE & Dang LX (1994) Computer-Simulations of Nacl Association in Polarizable Water. *Journal of Chemical Physics* 100(5):3757-3766.
10. Warr O, Ballentine CJ, Mu JJ, & Masters A (2015) Optimizing Noble Gas-Water Interactions via Monte Carlo Simulations. *Journal of Physical Chemistry B* 119(45):14486-14495.
11. FrenKel D & Smit B (2002) *Understanding molecular simulation from algorithms to applications* (Academic Press, New York).
12. Moultos OA, Tsimpanogiannis IN, Panagiotopoulos AZ, & Economou IG (2014) Atomistic Molecular Dynamics Simulations of CO2 Diffusivity in H2O for a Wide Range of Temperatures and Pressures. *Journal of Physical Chemistry B* 118(20):5532-5541.
13. Versteeg GF & Vanswaaij WPM (1988) Solubility and Diffusivity of Acid Gases (Co2, N2o) in Aqueous Alkanolamine Solutions. *J Chem Eng Data* 33(1):29-34.
14. Jahne B, Heinz G, & Dietrich W (1987) Measurement of the Diffusion-Coefficients of Sparingly Soluble Gases in Water. *J Geophys Res-Oceans* 92(C10):10767-10776.

15. Rao Q & Leng YS (2016) Molecular Understanding of CO_2 and H_2O in a Montmorillonite Clay Interlayer under CO_2 Geological Sequestration Conditions. *J Phys Chem C* 120(5):2642-2654.
16. Kim JS, Wu Z, Morrow AR, Yethiraj A, & Yethiraj A (2012) Self-Diffusion and Viscosity in Electrolyte Solutions. *Journal of Physical Chemistry B* 116(39):12007-12013.
17. Panagiotopoulos AZ, Quirke N, Stapleton M, & Tildesley DJ (1988) Phase-Equilibria by Simulation in the Gibbs Ensemble - Alternative Derivation, Generalization and Application to Mixture and Membrane Equilibria. *Mol Phys* 63(4):527-545.
18. Martin MG (2013) MCCCS Towhee: a tool for Monte Carlo molecular simulation. *Mol Simulat* 39(14-15):1184-1194.
19. Metropolis N, Rosenbluth AW, Rosenbluth MN, Teller AH, & Teller E (1953) Equation of State Calculations by Fast Computing Machines. *Journal of Chemical Physics* 21(6):1087-1092.
20. Smith S (1985) Noble gas solubility in water at high temperature. *Eos* 66:397.
21. Vorholz J, Harismiadis VI, Rumpf B, Panagiotopoulos AZ, & Maurer G (2000) Vapor plus liquid equilibrium of water, carbon dioxide, and the binary system, water plus carbon dioxide, from molecular simulation. *Fluid Phase Equilibr* 170(2):203-234.
22. Berendsen HJC, Postma JPM, Gunsteren WFv, & Hermans J (1981) Intermolecular Forces ed Pullman BReidel, Dordrecht).
23. Harris JG & Yung KH (1995) Carbon Dioxides Liquid-Vapor Coexistence Curve and Critical Properties as Predicted by a Simple Molecular-Model. *J Phys Chem-Us* 99(31):12021-12024.
24. Liu Y, Panagiotopoulos AZ, & Debenedetti PG (2011) Monte Carlo Simulations of High-Pressure Phase Equilibria of CO_2-H_2O Mixtures. *Journal of Physical Chemistry B* 115(20):6629-6635.
25. Hou SX, Maitland GC, & Trusler JPM (2013) Measurement and modeling of the phase behavior of the (carbon dioxide plus water) mixture at temperatures from 298.15 K to 448.15 K. *J Supercrit Fluid* 73:87-96.